

Enhanced adsorption of phthalic acid from aqueous solution by LDH@ZIF-8 composites

Yingwei Wang^a, Yingli Yang^b, Xinlong Yan^{b,*}

^aSinopec Petroleum Engineering Corporation, Shandong Provincial Key Laboratory for Treatment of Oilfield Produced Water and Environmental Pollution, Dongying 257026, China, email: wangyw.osec@sinopec.com

^bCollege of Chemical Engineering, China University of Mining & Technology, Xuzhou 221116, China, emails: yanxl@cumt.edu.cn (X. Yan)

Received 10 May 2023; Accepted 12 August 2023

ABSTRACT

LDH@ZIF-8 composite has been synthesized via *in-situ* growth of zeolitic imidazolate frameworks-8 (ZIF-8) on Zn/Al hydrotalcite. The morphology and composition of the samples were characterized by X-ray diffraction, Fourier-transform infrared spectroscopy, scanning electron microscope and N₂ adsorption-desorption techniques. The adsorption performances of LDH@ZIF-8 sample for phthalic acid were investigated. The results show that the adsorption capacity of LDH@ZIF-8 could be as high as 508.72 mg/g at 20°C, C₀ = 100 mg/g. The adsorption isotherms and adsorption kinetics were well described by Freundlich isotherm model and the pseudo-first-order kinetic equation, respectively. In addition, recycling experiments revealed that the behavior of LDH@ZIF-8 is maintained after recycling for at least three times.

Keywords: Hydrotalcite; Zeolitic imidazolate frameworks (ZIFs); *In-situ* synthesis; Adsorption; Phthalic acid

1. Introduction

In recent years, with the rapid development of chemical and related industries in the world, the problem of water pollution caused behind industrialization has become increasingly serious [1]. Phthalates, a common class of plasticizers, are extensively used in plastic production. Their products are widely distributed in various industries, posing a risk of migration into the water environment. Due to their metabolism, they can easily accumulate in water, leading to significant water pollution issues [2]. Therefore, the efficient treatment of phthalic acid-containing wastewater has become an urgent environmental problem in the world today.

Usually, there are various methods used for the treatment of phthalic acid in water, such as biodegradation, adsorption separation, oxidative degradation, etc [3,4]. The adsorption method offers a broad range of application prospects due to

its advantages of simple operation and low energy consumption. The key factor in achieving these prospects lies in the development of highly efficient adsorbents. Zeolitic imidazolate frameworks (ZIFs), as a new class of metal-organic frameworks (MOFs), are metal-organic skeletal materials formed by assembling with divalent metals (Zn²⁺, Co²⁺, etc.) using organic imidazole esters or their derivatives as linking ligands, with a structure similar to that of traditional zeolite molecular sieves [5]. ZIFs not only inherit the advantages of MOFs, but also overcome the disadvantages of poor thermal and chemical stability of MOFs to a certain extent, and have broad application prospects in fields such as adsorption. However, the high cost of ZIFs and the fact that they are mostly nanoparticles, which are difficult to be separated after adsorption in water, limit their large-scale applications.

Hydrotalcite layered double hydroxide (LDH) is a typical class of anionic layered compounds consisting of positively charged laminates and interlayer filled with

* Corresponding author.

negatively charged anions, with variable composition of metal ions on the main laminate, charge of the main laminate, type and number of intercalating anions [6]. Due to its unique physicochemical properties, hydrotalcite has been studied extensively by many researchers and has been widely used in the field of adsorption in recent years [7]. However, hydrotalcite itself has a weak adsorption capacity for phthalic acid; therefore, modification of hydrotalcite to improve its adsorption capacity is of great importance for phthalic acid removal.

Considering that the hydrotalcite structure contains divalent metals that can be combined with organic imidazole ligands, the *in-situ* synthesis of ZIFs on the surface of LDH is expected to improve the utilization efficiency of ZIFs and reduce the cost of adsorbents. At the same time, the combination of the two materials can also make the adsorbent easy to separate due to the large size of hydrotalcite particles. Therefore, in this work, Zn-Al LDH was synthesized by co-precipitation method, and zeolitic imidazolate frameworks-8 (ZIF-8) was synthesized *in-situ* on the surface of Zn-Al LDH. The adsorption capacity of ZIF-8, Zn-Al LDH and LDH@ZIF-8 samples toward phthalic acid was analyzed and compared, and the adsorption performance of LDH@ZIF-8 was further studied in-depth. The primary investigations encompass the performances of thermodynamic, kinetic, and adsorption cycles, which provide new ideas for the preparation of modified hydrotalcite adsorbents and the removal of phthalic acid from water.

2. Experimental set-up

2.1. Materials

Aluminum nitrate ($\text{Al}(\text{NO}_3)_3 \cdot 9\text{H}_2\text{O}$), zinc nitrate ($\text{Zn}(\text{NO}_3)_2 \cdot 6\text{H}_2\text{O}$), sodium hydroxide (NaOH), sodium formate (HCOONa), 2-methylimidazole (2-MIm), triethylamine (TEA), methanol (CH_3OH) and hydrochloric acid (HCl) were obtained from Sinopharm Chemical Reagent Co. All solvents and chemicals are of analytical reagent grade and were used without further purification.

2.2. Synthesis of LDH@ZIF-8

2.2.1. Preparation of LDHs

3.57 g of $\text{Zn}(\text{NO}_3)_2 \cdot 6\text{H}_2\text{O}$ and 1.13 g of $\text{Al}(\text{NO}_3)_3 \cdot 9\text{H}_2\text{O}$ were added to deionized water and mixed under constant stirring to form a solution, with a metal ion concentration of 0.15 mol/L. The pH of the solution was then adjusted with sodium hydroxide (2 M) to keep it at ~7.5. Finally, the above solution was transferred into a three-mouth flask and heated in a water bath at 70°C for 24 h. After the solution cooled down, a white precipitate was collected by centrifugation and washing and dried at 70°C, and the resulting sample was labeled as Zn-Al LDH.

2.2.2. Preparation of LDH@ZIF-8

0.75 g of 2-methylimidazole and 0.405 g of sodium formate were dissolved in 60 mL of methanol, then 0.36 g of Zn-Al LDH sample was added to the above solution. The mixture was stirred at room temperature for a few minutes,

and then heated at a constant temperature of 60°C for 4 h. Finally, the solution was cooled, centrifuged, washed and collected to obtain a white sample. After dried at 50°C, the resulting sample was labeled as LDH@ZIF-8.

2.3. Characterization

Powder X-ray diffraction (XRD) patterns of all samples were recorded on a Bruker D8 ADVANCE diffractometer (Germany) with Cu KR radiation (40 kV, 30 mA). The N_2 adsorption-desorption isotherms were collected at 77 K using IQ2 Quantachrome porosimeter. Prior to the measurement, the samples were degassed at 150°C overnight. The total pore volume was determined as the volume of liquid nitrogen adsorbed at a relative pressure of 0.99. The micropore volume (V_{micro}) was estimated using *t*-plot method and mesopore volumes were obtained by subtracting V_{micro} from the total pore volume. Fourier-transform infrared (FTIR) spectra were collected on a Nicolet iS5 Spectrometer (Thermo Fisher Scientific, USA) in the range of 4,000–400 cm^{-1} with a 2 cm^{-1} resolution. The morphology of the samples was collected by scanning electron microscope (FEI Quanta 400 FEG, USA). Transmission electron microscope investigation of morphological features was performed using a FEI Tecnai G2 F20 device operated at 200 kV.

2.4. Adsorption removal of phthalic acid

2.4.1. Adsorption thermodynamic experiments

5 mg of vacuum-dried adsorbents (Zn-Al LDH, ZIF-8, LDH@ZIF-8) were added into 50 mL of phthalic acid solution and stirred at constant temperature for 24 h. Then, the solutions were filtered with 0.22 μm polytetrafluoroethylene (PTFE) membrane filters and the absorbance of the adsorbed solution was measured with a UV spectrophotometer (Beijing Pu-Analysis, TU-1810) at 280 nm. The adsorption capacity were calculated through Eq. (1):

$$q_e = \frac{(C_0 - C_e)V}{m} \quad (1)$$

where C_0 and C_e are the mass concentrations of adsorbent in the solution at the initial and adsorption equilibrium (mg/L), respectively; V is the volume of solution (L); m is the mass of adsorbent (g); q_e is the adsorption capacity at adsorption equilibrium (mg/g).

2.4.2. Kinetic adsorption experiment

100 mL of phthalic acid solution with a concentration of 100 mg/L was mixed with 10 mg of vacuum-dried adsorbent and stirred continuously, and the temperature was kept at 20°C. At certain intervals, a certain amount of the solution was taken and filtered through a 0.22 μm PTFE membrane filter, and then the absorbance of the solution was measured by a UV spectrophotometer, and the adsorption capacity at time t were calculated [Eq. (2)].

$$q_t = \frac{(C_0 - C_t)V}{m} \quad (2)$$

where C_0 and C_t are the mass concentration of adsorbent in solution at initial and adsorption time of t , respectively (mg/L); V is the volume of solution (L); m is the mass of adsorbent (g); q_t is the adsorption amount at the adsorption time of t (mg/g).

3. Results and discussion

3.1. Characterization of LDH@ZIF-8

Fig. 1 shows the XRD patterns of the ZIF-8, Zn-Al LDH and LDH@ZIF-8 samples. It can be seen that the ZIF-8 material shows diffraction peaks at 2θ degree of 7° , 10° , 12° , 14° , 18° , 22° , 24° , 26° and 29° , which are consistent with the characteristic diffraction peaks of ZIF-8 [8]. For Zn-Al LDH, the diffraction peaks appeared at 11.7° , 23.6° , 34.6° , indicating the successful synthesis of Zn-Al LDH. The XRD pattern of LDH@ZIF-8 contains the characteristic diffraction peaks of ZIF-8 and no other peaks can be observed, indicating the successfully synthesis of ZIF-8 with Zn-Al LDH.

Fig. 2 shows the FTIR spectra of ZIF-8, Zn-Al LDH and LDH@ZIF-8 samples before and after the adsorption of phthalic acid. The spectra of the samples without phthalic acid adsorption are revealed in Fig. 2a–c, the absorption peaks at $3,450$ and $1,610$ cm^{-1} are generated by hydroxyl stretching vibration and water molecule bending vibration. The absorption peaks at $1,760$; $1,370$ and $1,370$ cm^{-1} for Zn-Al LDH samples was ascribed to the interlayer NO_2^- stretching vibration and interlayer M–O, M–O–M bending vibration, respectively, and the absorption peak at $2,400$ cm^{-1} was attributed to interlayer CO_3^{2-} ion [9]. For ZIF-8 sample, different absorption peaks at $3,450$; $3,130$; $2,950$; $1,610$ and 500 – $1,500$ cm^{-1} could be observed, which corresponding to the stretching vibration of –OH in solvent methanol, C–H stretching vibration of methyl, C–H stretching vibration of imidazole ring, bending vibration of –OH and stretching and bending vibration on imidazole ring, respectively [10]. As for LDH@ZIF-8, it can be seen that the same absorption peaks as ZIF-8 exist at $3,450$; $3,130$; $2,950$; $1,610$ and below $1,500$ cm^{-1} [11,12], indicating the presence of ZIF-8 on the surface of Zn-Al LDH sample, which is consistent with the

results of XRD analysis. After phthalic acid adsorption, the peaks at $3,450$; $2,840$; $1,580$; $1,410$ and 751 cm^{-1} are the absorption peaks of –OH, –COOH stretching vibration and –OH bending vibration (Fig. 2d–f), respectively. The peaks near $1,580$ cm^{-1} were attributed to the C=C stretching vibration on the benzene ring, and the absorption peak at 751 cm^{-1} corresponded to the stretching vibration of the neighboring substituent on the benzene ring. The above results confirms that phthalic acid has been adsorbed by ZIF-8, Zn-Al LDH and LDH@ZIF-8 samples.

The morphologies of ZIF-8, Zn-Al LDH and LDH@ZIF-8 samples are shown in Fig. 3. It can be seen that ZIF-8 was a nanoparticle with a size of ~ 10 nm (Fig. 3a). The Zn-Al LDH sample (Fig. 3c) exhibits a scale-like structure with a smoother surface. Compared with the morphological structure of Zn-Al LDH, the LDH@ZIF-8 sample (Fig. 3d) has a rough surface and presence of nanoparticles with a rhombic dodecahedral structure on its surface [13,14], indicating that ZIF-8 was grown *in-situ* on the Zn-Al LDH surface.

The pore structures of ZIF-8, Zn-Al LDH and LDH@ZIF-8 samples were characterized by N_2 adsorption/desorption technics, and the adsorption isotherms are shown in Fig. 4. The isotherm of Zn-Al LDH belongs to a type IV and has hysteresis loops, indicating that the synthesized material has a mesoporous structure [15,16]. Between the relative pressures of 0.1 – 0.8 , the nitrogen adsorption is essentially constant and the isotherms are close to horizontal, indicating that multilayer adsorption occurs. When the relative pressure continues to increase, the nitrogen adsorption tends to increase significantly, indicating that it has large particle stacking pores. The adsorption isotherm of ZIF-8 belongs to a mixture of types I and IV and have hysteresis loop, providing its microporous structure contains a small amount of mesoporous structure [17]. Similarly, the adsorption isotherm of LDH@ZIF-8 sample belongs to the mixed type I and IV with hysteresis loops. At low relative pressures, the nitrogen adsorption capacity increases rapidly due to their microporous structure. With the increase of relative pressure, the N_2 adsorption tends to level off. When the relative

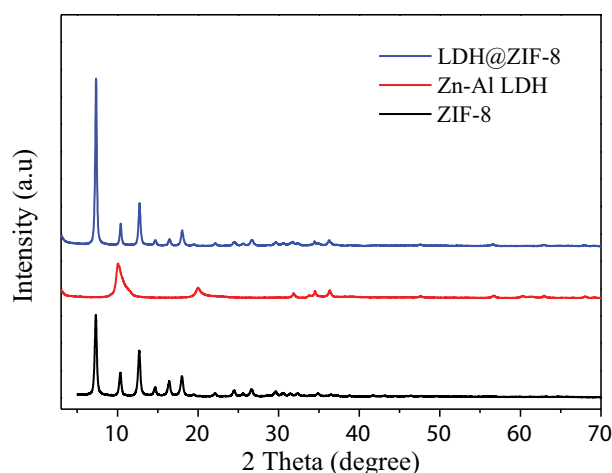


Fig. 1. X-ray diffraction patterns of ZIF-8, Zn-Al LDH and LDH@ZIF-8 samples.

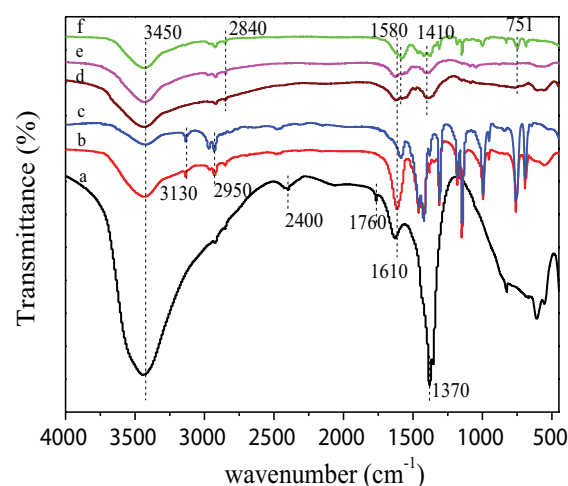


Fig. 2. Fourier-transform infrared spectra of ZIF-8, Zn-Al LDH and LDH@ZIF-8 samples (a–c); ZIF-8 (H_2 -PA), LDH@ZIF-8 (H_2 -PA) and Zn-Al LDH (H_2 -PA) (d–f).

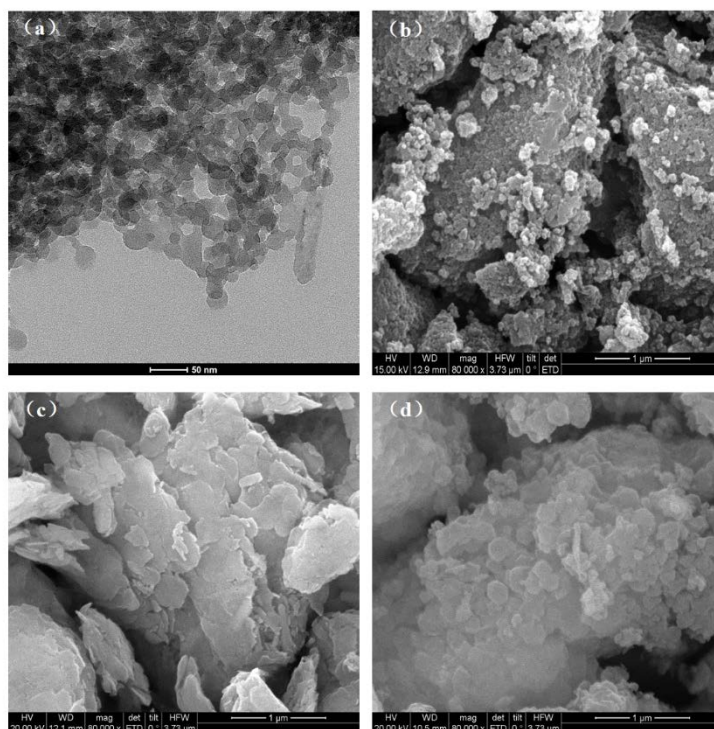


Fig. 3. Transmission electron microscope image of ZIF-8 (a) and scanning electron microscope images of ZIF-8, Zn-Al LDH and LDH@ZIF-8 (b–d), respectively.

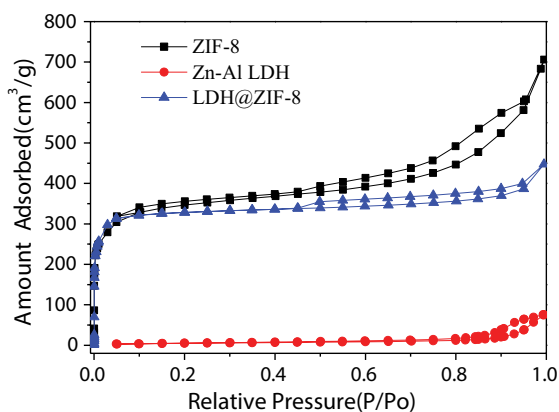


Fig. 4. Nitrogen adsorption–desorption isotherms of ZIF-8, Zn-Al LDH and LDH@ZIF-8 samples.

pressure approaches 1, the isotherm shows an increasing trend again, indicating that there are a large amount of macroporous structures in the composite sample [18]. The Brunauer–Emmett–Teller surface area (1,240 m²/g) and pore volume (0.69 cm³/g) of the LDH@ZIF-8 composite are lower than those of ZIF-8 (1,320 m²/g and 1.06 cm³/g) (Table 1), but much higher than that of LDH, which also indicates the combination of ZIF-8 and LDH in the LDH@ZIF-8 sample.

3.2. Adsorption isotherms and kinetics

Phthalic acid was selected as the adsorbent, and the synthesized samples were used as adsorbent. The adsorption

Table 1

Surface area and pore structure of ZIF-8, Zn-Al LDH and LDH@ZIF-8 samples

Samples	S_{BET} (m ² /g)	S_{Langmuir} (m ² /g)	V_t (cm ³ /g)	V_{meso} (cm ³ /g)	V_{micro} (cm ³ /g)
Zn-Al LDH	17.9	28.61	0.12	0.12	0
ZIF-8	1,320.1	1,712.89	1.06	0.64	0.42
LDH@ZIF-8	1,242	1,471.93	0.69	0.22	0.47

results at different initial concentrations were shown in Fig. 5. After the adsorption equilibrium reached, it can be seen that the adsorption capacity of LDH@ZIF-8 at an initial concentration of 100 mg/L is much greater than that of Zn-Al LDH (359.64 mg/g), which is comparable to that of pure ZIF-8 (about 510 mg/g). In terms of the amount of phthalic acid adsorbed per square meter, LDH@ZIF-8 shows an even higher value compared to that of ZIF-8 (Fig. 5b). This is due to the fact that the *in-situ* growth of ZIF-8 onto the surface of Zn-Al LDH facilitates the dispersion of ZIF-8, while the positively charged surface of ZIF-8 adsorbs with the anion of phthalic acid through electrostatic interaction. In addition, the interlayer anion exchange property possessed by Zn-Al LDH can also promote the adsorption. The adsorption capacities of several potential adsorbents for the removal of phthalic acid, as well as LDH@ZIF-8, are provided in Table 2. It has been found that LDH@ZIF-8 exhibits significantly higher adsorption capacity compared to activated carbon, UIO-66, and UIO-67 adsorbents, and similar

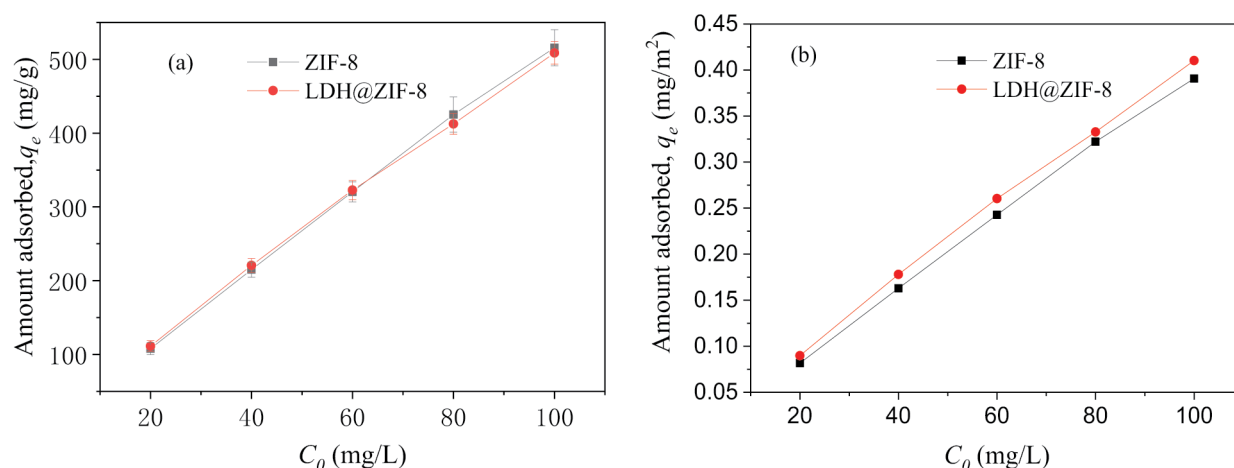


Fig. 5. (a) Comparison of ZIF-8 and LDH@ZIF-8 for the adsorption of phthalic acid (mg/g) at different initial concentrations and (b) comparison of ZIF-8 and LDH@ZIF-8 adsorption capacities based on their surface area capacities (mg/m²).

Table 2

Comparison of adsorption performance of LDH@ZIF-8 with the reported adsorbent

Adsorbents	Temperature (°C)	Equilibrium time (h)	Initial H ₂ -PA concentration (mg/L)	Adsorption capacity (mg/g)	References
Activated carbon	25	12	100	249	[19]
UIO-66	25	12	100	187	[19]
MAF-6	20	2	100	572	[20]
UIO-67	25	1	100	434	[21]
LDH@ZIF-8	20	2	100	508	This work

performance to the MAF-6 adsorbent. Moreover, after the combination of ZIFs and LDH, the particle size of the sample increases significantly, which is favorable for the separation. Therefore, LDH@ZIF-8 can be a promising adsorbent for the removal of phthalic acid from aqueous solutions, thus, the process of phthalic acid adsorption by LDH@ZIF-8 was further investigated.

The adsorption capacity of LDH@ZIF-8 on phthalic acid was further investigated by varying the initial concentration and temperature, and the results are shown in Fig. 6. It can be seen that the equilibrium adsorption capacity of LDH@ZIF-8 gradually increased with the increase of the initial concentration of phthalic acid. However, the adsorption capacity decreased slightly with the increase of temperature, indicating that the increase of temperature was not favorable for the adsorption. The thermodynamic data were fitted with the Langmuir isothermal adsorption model and Freundlich isothermal adsorption model [22,23], respectively, and the fitting results are shown in Fig. 7 and Table 3. As seen in Table 3, the linear correlation coefficients of the Freundlich isothermal adsorption model were larger than those of the Langmuir isothermal adsorption model at different temperatures, indicating that the thermodynamic adsorption process of LDH@ZIF-8 for phthalic acid was more consistent with the Freundlich isothermal adsorption model, and multilayer adsorption may occur in the adsorption process. In addition, the thermodynamic parameters of the adsorption process were analyzed by using Eqs.

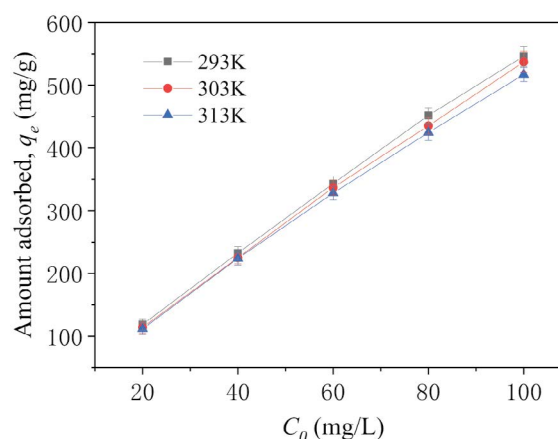


Fig. 6. Effect of adsorption temperature on the adsorption of phthalic acid by LDH@ZIF-8.

(3)–(5), and the results are shown in Table 4. It can be seen that ΔG is less than 0 during the adsorption process, which indicates that the adsorption is spontaneous; ΔH (−4.43 kJ/mol) is less than 0 and has a small value, which reveals that the adsorption is an exothermic physisorption process. Therefore, the increase in temperature is not favorable for the stable adsorption of phthalic acid on the surface of the LDH@ZIF-8.

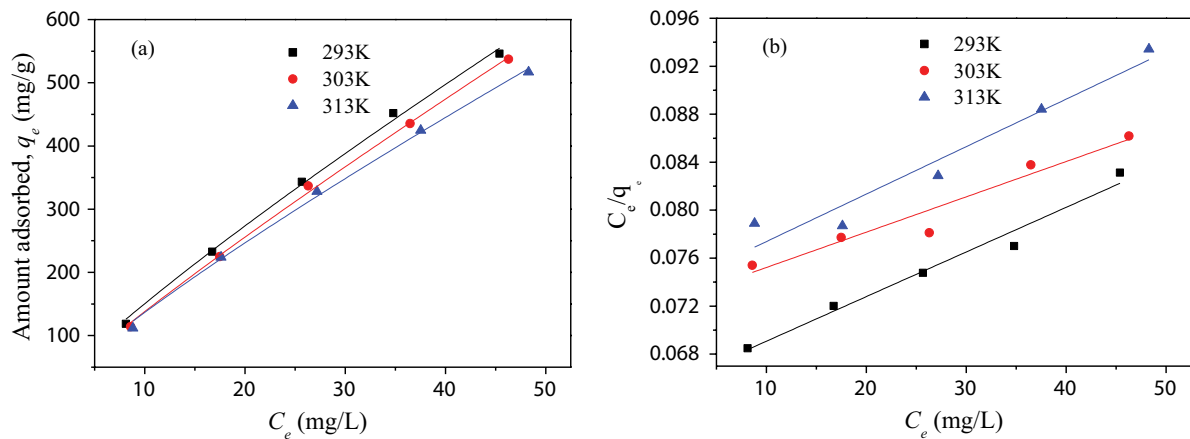


Fig. 7. Langmuir (a) and Freundlich (b) fitting curves for the adsorption of phthalic acid by LDH@ZIF-8.

Table 3
Langmuir and Freundlich isotherm parameters of phthalic acid adsorption by LDH@ZIF-8

LDH@ZIF-8	Langmuir isothermal model			Freundlich isothermal model		
	k_L (L/mg)	q_m (mg/g)	R^2	k_F (mg/g)	n	R^2
293 K	0.00569	2,688.37	0.9706	20.65615	1.1596	0.9970
303 K	0.00407	3,396.51	0.9234	17.74862	1.1163	0.9981
313 K	0.00539	2,527.52	0.9235	19.22785	1.1741	0.9970

Table 4
Thermodynamic parameters at different temperatures (K_c calculated at an initial concentration of 100 mg/L)

Temperature (K)	K_c	ΔG (kJ/mol)	ΔH (kJ/mol)	ΔS (J/(mol·K))
293 K	12.03	-6.08		
303 K	11.60	-6.13	-4.43	5.61
313 K	10.70	-6.19		

$$K_c = \frac{q_e}{C_e} \quad (3)$$

$$\Delta G = -RT \ln K_c = \Delta H - T\Delta S \quad (4)$$

$$\ln K_c = \frac{\Delta S}{R} - \frac{\Delta H}{RT} \quad (5)$$

where q_e : equilibrium adsorption capacity (mg/g); C_e : equilibrium adsorption concentration (mg/L); ΔG : Gibbs free energy of adsorption (kJ/mol); ΔH : enthalpy change during adsorption (kJ/mol); ΔS : entropy change during adsorption (J/(mol·K)); T : adsorption temperature (K); R : molar constant of gas (8.314 J/(mol·K)).

The relationship between the adsorption time and the adsorption capacity of LDH@ZIF-8 was investigated in a solution of phthalic acid at 20°C and an initial concentration of 100 mg/g, and the results are shown in Fig. 8. It can

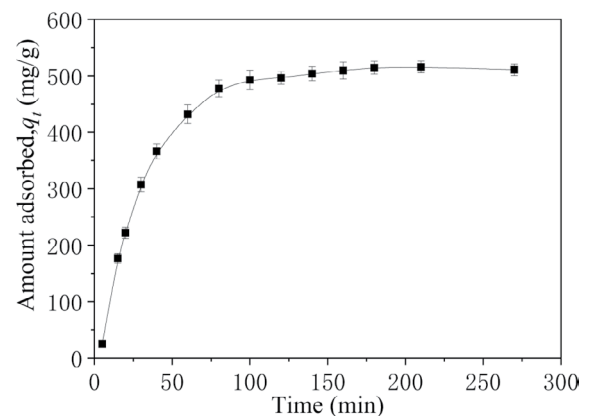


Fig. 8. Adsorption of phthalic acid by LDH@ZIF-8 sample at different adsorption times.

be seen that the adsorption capacity increased rapidly with the increase of adsorption time within 60 min, indicating that the adsorption sites on LDH@ZIF-8 were occupied by phthalic acid rapidly. Then, the adsorption capacity increased slowly until the adsorption equilibrium was reached. For the above results, pseudo-first-order, pseudo-second-order and intraparticle diffusion equations [24,25] were fitted, and the fitting results are shown in Fig. 9 and Table 5.

From the results (Table 5), it can be seen that the linear correlation coefficient of the pseudo-first-order kinetic fit ($R^2 = 0.991$) is slightly larger than that of the pseudo-second-order kinetic fit ($R^2 = 0.908$), and the calculated values of equilibrium adsorption are basically close to the

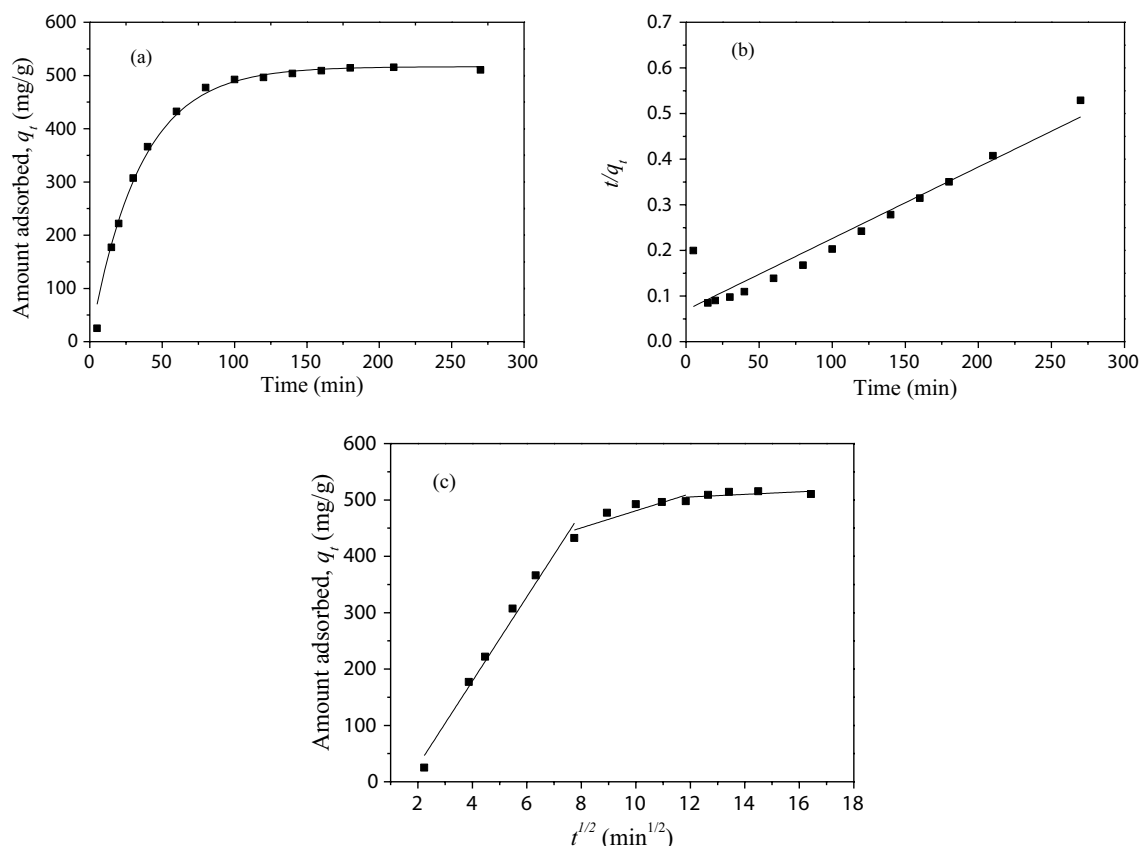


Fig. 9. Pseudo-first-order kinetic model (a), pseudo-second-order kinetic model (b) and intraparticle diffusion model fitting curves (c) of phthalic acid adsorption by LDH@ZIF-8 samples.

Table 5

Pseudo-first-order kinetic and pseudo-second-order kinetic fitting parameters for the adsorption of phthalic acid by LDH@ZIF-8 samples

Sample	$q_{e,exp}$ (mg/g)	Pseudo-first-order kinetic model			Pseudo-second-order kinetic model		
		k_1 (min^{-1})	q_e (mg/g)	R^2	k_2 ($\text{g}/(\text{mg}\cdot\text{min})$)	q_e (mg/g)	R^2
LDH@ZIF-8	508.7	0.02927	515.687	0.991	3.5584×10^{-5}	636.943	0.908

experimental values. Therefore, the adsorption of phthalic acid by LDH@ZIF-8 samples was more consistent with the pseudo-second-order kinetic model. The fitted curve of intraparticle diffusion (Fig. 9c) does not pass through the origin, indicating that the internal diffusion is not the only control step in the adsorption process. In the fitted curve, the adsorption process can be divided into three stages. Stage I: the steep slope of the straight line indicates that the adsorption rate is faster in this stage, which attributed to abundance of active sites on the adsorbent surface. These active are quickly occupied by the adsorbate. Stage II: the adsorption rate depends on the diffusion of phthalic acid molecules within the pores of LDH@ZIF-8, and smaller slope of the curve indicates that phthalic acid with larger molecular size is more difficult to into the pores of LDH@ZIF-8. As a result, adsorption rate is slower. Stage 3: the curve appears to be almost horizontal, indicating that the process of adsorption has reached saturation [26].

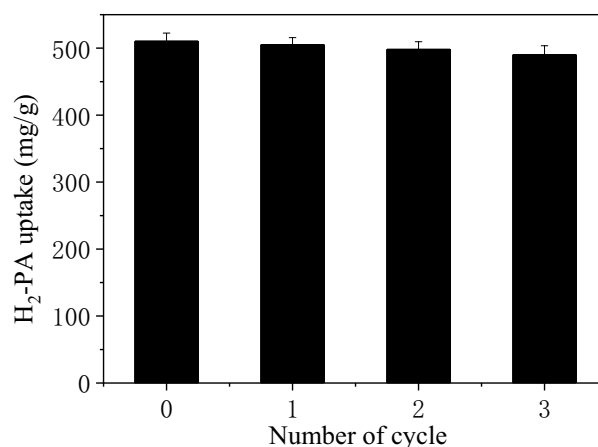


Fig. 10. Recyclability of LDH@ZIF-8 for the adsorption of phthalic acid.

After the adsorption test, the adsorbent was filtered and treated with low concentration of sodium hydroxide (0.01 mol/L) to desorb the adsorbate. The treated sample was then dried and re-used for the adsorption of phthalic acid. The adsorption cycling performance of LDH@ZIF-8 on phthalic acid is shown in Fig. 10. It can be seen that the adsorption capacity of LDH@ZIF-8 on phthalic acid remained at a high level, and the adsorption capacity could reach more than 95% of the initial adsorption capacity after three cycles of adsorption, indicating that LDH@ZIF-8 has good stability and can be recycled for many times.

4. Conclusion

In this work, ZIF-8 was synthesized on the surface of Zn-Al LDH by an *in-situ* synthesis method. After conducting XRD, FTIR, and morphological analyses, it was determined that ZIF-8 was successfully synthesized on the surface of Zn-Al LDH. Additionally, the composite surface displayed a rhombic dodecahedral structure composed of ZIF-8 particles. Under the same conditions, the adsorption capacity of LDH@ZIF-8 for phthalic acid was greater than that of Zn-Al LDH and comparable to that of pure ZIF-8, however, the adsorption capacity per unit area was better than that of pure ZIF-8. The adsorption isotherms of LDH@ZIF-8 were found to be in good agreement with the Freundlich isothermal adsorption model. Furthermore, the adsorption capacity exhibited a decreasing trend as the temperature increased. This suggests that the adsorption process is exothermic and involves multilayer physical adsorption. The adsorption kinetics were better suited to fit the pseudo-first-order kinetic model. After three cycles of adsorption, the LDH@ZIF-8 still maintained a high adsorption capacity of 500 mg/g, with adsorption capacity losses consistently below 5%.

Declaration of competing interest

The authors declare that they have no known competing financial interests or personal relationships that could have appeared to influence the work reported in this paper.

Acknowledgments

This work was supported by the Open Research Fund Program of Shandong Province Key Laboratory of Oilfield Produced Water Treatment and Environmental Pollution Control (ZY2021009) and the Key Research and Development Program of Xuzhou, China (Grant KC19214).

References

- [1] K. Kümmerer, D.D. Dionysiou, O. Olsson, D.A. Fatta-Kassinos, path to clean water, *Science*, 361 (2018) 222–224.
- [2] H.T. Tran, C. Lin, X.-T. Bui, M.K. Nguyen, N.D.T. Cao, H. Mukhtar, H.G. Hoang, S. Varjani, H.H. Ngo, L.D. Nghiem, Phthalates in the environment: characteristics, fate and transport, and advanced wastewater treatment technologies, *Bioresour. Technol.*, 344 (2022) 126249, doi: 10.1016/j.biortech.2021.126249.
- [3] J.-R. Feng, Q.-X. Deng, H.-G. Ni, Photodegradation of phthalic acid esters under simulated sunlight: mechanism, kinetics, and toxicity change, *Chemosphere*, 299 (2022) 134475, doi: 10.1016/j.chemosphere.2022.134475.
- [4] Y.-H. Xiong, D.-S. Pei, A review on efficient removal of phthalic acid esters *via* biochars and transition metals-activated persulfate systems, *Chemosphere*, 277 (2021) 130256, doi: 10.1016/j.chemosphere.2021.130256.
- [5] J.O. Ighalo, S. Rangabhashiyam, C.A. Adeyanju, S. Ogunniyi, A.G. Adeniyi, C.A. Igwegbe, Zeolitic imidazolate frameworks (ZIFs) for aqueous phase adsorption—a review, *J. Ind. Eng. Chem.*, 105 (2022) 34–48.
- [6] M. Zubair, M. Daud, G. McKay, F. Shehzad, M.A. Al-Harthi, Recent progress in layered double hydroxides (LDH)-containing hybrids as adsorbents for water remediation, *Appl. Clay Sci.*, 143 (2017) 279–292.
- [7] P.M. Bodhankar, P.B. Sarawade, G. Singh, A. Vinu, D.S. Dhawale, Recent advances in highly active nanostructured NiFe LDH catalyst for electrochemical water splitting, *J. Mater. Chem. A*, 9 (2021) 3180–3208.
- [8] H. Jiang, Q. Yan, R. Chen, W. Xing, Synthesis of Pd@ZIF-8 via an assembly method: influence of the molar ratios of Pd/Zn²⁺ and 2-methylimidazole/Zn²⁺, *Microporous Mesoporous Mater.*, 225 (2016) 33–40.
- [9] A.A. Ali Ahmed, Z.A. Talib, M.Z. bin Hussein, A. Zakaria, Zn-Al layered double hydroxide prepared at different molar ratios: preparation, characterization, optical and dielectric properties, *J. Solid State Chem.*, 191 (2012) 271–278.
- [10] M.M. Liu, W.M. Lv, X.F. Shi, B.B. Fan, R.F. Li, Characterization and catalytic performance of zeolitic imidazolate framework-8 (ZIF-8) synthesized by different methods, *Chin. J. Inorg. Chem.*, 30 (2014) 579–584.
- [11] K. Kida, M. Okita, K. Fujita, S. Tanaka, Y. Miyake, Formation of high crystalline ZIF-8 in an aqueous solution, *CrystEngComm*, 15 (2013) 1794–1801.
- [12] Z. Abbasi, E. Shamsaei, X. Fang, B. Ladewig, H. Wang, Simple fabrication of zeolitic imidazolate framework ZIF-8/polymer composite beads by phase inversion method for efficient oil sorption, *J. Colloid Interface Sci.*, 493 (2017) 150–161.
- [13] B.J. Joshua, Y.S. Lin, Kinetics of ZIF-8 thermal decomposition in inert, oxidizing, and reducing environments, *J. Phys. Chem. C*, 120 (2016) 14015–14026.
- [14] X. Yan, Y. Yang, C. Wang, X. Hu, M. Zhou, S. Komarneni, Synthesis of pore-expanded mesoporous ZIF-8/silica composites in the presence of swelling agent, *J. Sol-Gel Sci. Technol.*, 81 (2017) 268–275.
- [15] B. Han, G. Cheng, E. Zhang, L. Zhang, X. Wang, Three dimensional hierarchically porous ZIF-8 derived carbon/LDH core-shell composite for high performance supercapacitors, *Electrochim. Acta*, 263 (2018) 391–399.
- [16] C. Wang, R. Zhang, Y. Miao, Q. Xue, B. Yu, Y. Gao, Z. Han, M. Shao, Preparation of LDO@TiO₂ core-shell nanosheets for enhanced photocatalytic degradation of organic pollution, *Dalton Trans.*, 50 (2021) 17911–17919.
- [17] W. Meng, H. Wu, X. Bi, Z. Huo, J. Wu, Y. Jiao, J. Xu, M. Wang, H. Qu, Synthesis of ZIF-8 with encapsulated hexachlorocyclotriphosphazene and its quenching mechanism for flame-retardant epoxy resin, *Microporous Mesoporous Mater.*, 314 (2021) 110885, doi: 10.1016/j.micromeso.2021.110885.
- [18] H.M.F. Freundlich, Over the adsorption in solution, *J. Phys. Chem.*, 57 (1906) 385–470.
- [19] N.A. Khan, B.K. Jung, Z. Hasan, S.H. Jhung, Adsorption and removal of phthalic acid and diethyl phthalate from water with zeolitic imidazolate and metal-organic frameworks, *J. Hazard. Mater.*, 282 (2015) 194–200.
- [20] C. Wang, X. Yan, X. Hu, M. Zhou, Z. Ni, Metal-azolate framework-6 for fast adsorption removal of phthalic acid from aqueous solution, *J. Mol. Liq.*, 223 (2016) 427–430.
- [21] Q. Liu, J. Ye, Y. Han, P. Wang, Z. Fei, X. Chen, Z. Zhang, J. Tang, M. Cui, X. Qiao, Defective UiO-67 for enhanced adsorption of dimethyl phthalate and phthalic acid, *J. Mol. Liq.*, 321 (2021) 114477, doi: 10.1016/j.molliq.2020.114477.
- [22] J. Wei, J. Xu, Y. Mei, Q. Tan, Chloride adsorption on amino-benzoate intercalated layered double hydroxides: kinetic, thermodynamic and equilibrium studies, *Appl. Clay Sci.*, 187 (2020) 105495, doi: 10.1016/j.clay.2020.105495.

- [23] Y.S. Ho, G. McKay, Pseudo-second-order model for sorption processes, *Process Biochem.*, 34 (1999) 451–465.
- [24] X. Zhang, L. Yan, J. Li, H. Yu, Adsorption of heavy metals by L-cysteine intercalated layered double hydroxide: kinetic, isothermal and mechanistic studies, *J. Colloid Interface Sci.*, 562 (2020) 149–158.
- [25] J. Zhang, X. Yan, X. Hu, R. Feng, M. Zhou, Direct carbonization of Zn/Co zeolitic imidazolate frameworks for efficient adsorption of Rhodamine B, *Chem. Eng. J.*, 347 (2018) 640–647.
- [26] R. Lamaria, B. Benotmanea, S. Mezalib, Zeolite imidazolate framework-11 for efficient removal of bromocresol green in aqueous solution, isotherm kinetics, and thermodynamic studies, *Desal. Water Treat.*, 224 (2021) 407–420.